GENERAL EXPERIMENTAL TECHNIQUE

SEMICONDUCTOR SOURCES AND DETECTORS OF SPIN-POLARIZED ELECTRONS IN RESEARCH OF RESONANCE SCATTERING OF ELECTRONS

© 2025 O. E. Tereshchenko[a,*], S. A. Pshenichnyuk[b,], N. L. Asfandiarov[b], R. G. Rakhmeev[b], V. A. Golyashov[a], V. S. Rusetski[a], V. V. Bakin[a], G. E. Scheibler[a], S. A. Rozhkov[a], D. A. Kustov[a]**

[a]A.V. Rzhanov Institute of Semiconductor Physics, Siberian Branch Russian Academy of Sciences Russia, Novosibirsk

[b]Institute of Physics of Molecules and Crystals of the Ufa Scientific Center Russian Academy of Sciences Russia, Ufa

**email: teresh@isp.nsc.ru*

***e-mail:sapsh@anrb.ru*

Received May 08, 2024

Revised May 28, 2024

Accepted July 08, 2024

Abstract. The results of the developed semiconductor source of spin-polarized electrons and spin detector are presented, as well as the concept of their integration into the method of dissociative electron capture spectroscopy (DECS) taking into account the required values of the electron beam parameters at which resonance scattering and dissociative capture are observed. The design of the setup for studying the resonance scattering of spin-polarized electrons by the DECS method is described, which will allow studying the intramolecular dynamics of isolated negative ions. The main goal of the development and manufacture of the setup is the possibility of using it to study the interaction of spin-polarized electrons with chiral molecules, which will allow experimental verification of the Wester-Ulbricht hypothesis on the origin of biological homochirality. In addition to this fundamental issue, the expected results of the proposed experiment are important for promising areas of spintronics, as well as for establishing the molecular mechanisms of various biological effects of enantiomers of pharmaceuticals.

DOI: 10.31857/S00328162250124e3

1. INTRODUCTION

The mechanism of electron scattering by atoms and molecules, responsible for various spin-dependent effects such as exchange scattering, spin-orbital interaction, or their combinations, can generally be established from the dependence of the scattering cross-section on the energy of incident electrons and Z of the target [1, 2]. There exists a class of targets that are significantly more complex – chiral molecules. In the simplest case of having only one asymmetric atom (chirality center) in the molecular structure, there are only two enantiomers that differ from each other as mirror reflections. Obviously, it is impossible to superimpose two enantiomers in space by any other symmetry operations. Such targets, due to their symmetry (or lack thereof), allow the observation of new unique scattering effects [3, 4]. In addition to theoretical predictions about the polarization of an initially unpolarized electron beam that has undergone elastic scattering on optically active molecules [5], the presence of two scattering effects inherent to chiral targets is noted: different magnitude of attenuation of longitudinally polarized electron beams and rotation of the spin of scattered electrons with initially transverse beam polarization [6]. As noted by the author of [6], the first effect is analogous to circular dichroism, while the second is analogous to the rotation of the plane of light polarization. It is important to note that the interaction of polarized electrons with chiral molecules provides indirect information about the origin of biological homochirality, primarily in connection with the Vester-Ulbricht hypothesis [7]. The hypothesis is that cosmic beta rays preferentially destroyed one part of prebiotic chiral molecules, leaving the opposite part to participate in molecular evolution. It can be assumed that the polarization dependence of electron scattering by chiral molecules thus provides indirect evidence for such a picture. However, the physical mechanisms causing asymmetry in the scattering of spin-polarized electrons have been practically unexplored experimentally.

There is only a limited number of experimental studies on spin effects occurring during elastic scattering of slow (units-tens of electron volts) electrons by chiral molecules, conducted to detect mirror asymmetry. Early results on the detection of spin effects for unsubstituted camphor molecules [8] were not confirmed by subsequent studies [9, 10], however, signal asymmetry in the scattering cross-section was established for camphor derivatives in the interaction energy range of 0.5–10 eV [10]. Later, asymmetry in the total scattering cross-section of spin-polarized electrons was demonstrated for halogen-substituted camphor molecules [11] using the electron transmission spectroscopy method [12]. However, in the context of testing the Vester-Ulbricht hypothesis, it is necessary to detect asymmetry in the fragmentation of enantiomers with different polarization of the primary electron beam, which can only be implemented using the electron dissociative attachment

spectroscopy (EDAS) method. Until now, only a single experiment has been conducted to study electron dissociative attachment to halogen-substituted camphor molecules, performed, however, using the electron transmission spectroscopy method, i.e., without mass selection of the resulting negative ions (NI) and with the ability to register only sufficiently intense NI currents [13, 14]. In these works, at almost the limit of experimental sensitivity, an asymmetry in the formation of halogen fragment NIs was demonstrated, which are the dominant decay channel of negative molecular ions of halogen-substituted camphor. However, the magnitude of the effect, poor statistics, and the absence of direct spin-dependent measurements did not allow for unambiguously confirming or refuting the Vester-Ulbricht hypothesis.

This paper presents the concept of a manufactured setup for studying resonant scattering and fragmentation of target molecules by the mechanism of dissociative electron capture using spin-polarized electrons, as well as results on the creation and study of properties of new spin-polarized sources and detectors of free electron spin based on semiconductor heterostructures and their integration into the DEA method. We note separately that such integration is being carried out for the first time; in particular, the methods and techniques for working with a beam of spin-polarized electrons described in this paper were not available to the authors of pioneering works [13,14].

2. SOURCE OF SPIN-POLARIZED ELECTRONS

Until now, the most common source of spin-polarized electrons has been a GaAs-based photocathode [15]. The photocathode operation is based on two phenomena: (1) the creation of non-equilibrium spin-polarized electrons in the conduction band due to the optical pumping effect [16] and (2) the reduction of the vacuum level at the surface below the bottom of the conduction band in the semiconductor bulk (effective negative electron affinity) due to surface activation with cesium and oxygen. One of the complex technical problems in studying the scattering of spin-polarized electrons on molecules is the limited lifetime of the GaAs photocathode – the source of spin-polarized electrons. It is well known that the GaAs photocathode is sensitive even to the residual atmosphere of the vacuum chamber. Thus, at a base pressure level of 10^{-10} Torr, the lifetime (degradation) of the photocathode can be hours, and it critically depends on the composition of the residual atmosphere. The use of high-pressure cells (0.5–1.0 mTorr) in the DEA method requires a high rate of differential pumping of the entire electron optics path and photocathode chamber; however, this does not fundamentally solve the problem of GaAs photocathode degradation. For this reason, it is necessary to use sources of spin-polarized electrons that are more resistant to the residual atmosphere of the vacuum chamber. One such source is a photocathode based on multi-alkali compounds.

Multi-alkali photocathodes are widely used as electron sources in various colliders [17], in electron multipliers and electro-optical converters. We have recently shown that a Na_2KSb-based photocathode is also an efficient source of spin-polarized electrons [18]. To create spin-polarized electrons in semiconductor structures, the phenomenon of optical orientation is used, the essence of which is the transfer of angular momentum from a photon to an electron during the absorption of circularly polarized light. It was found that the Na_2KSb compound has a band structure similar to that of GaAs, including the band gap value, and the optical orientation effect is also observed in this compound. The presence of the optical orientation (pumping) effect can be determined from measurements of circularly polarized photoluminescence [16].

Conducting research on spin-dependent photoemission properties of photocathodes generally requires an ultra-high vacuum chamber containing the material under study, an electron lens system, and an energy analyzer. This system can be simplified to a vacuum photodiode, the electrodes of which are the heterostructures under study, one of which can be a source and the other a detector of spin-polarized electrons (Fig. 1) [19, 20]. Previously, similar vacuum photodiodes with A^3B^5 heterostructures had already been manufactured and the convenience of this system for studying the emission and injection properties of materials was demonstrated [21, 22]. The photodiode is a cylindrical body with a diameter of 30 mm and a height of 10-15 mm, made of aluminum oxide ceramics, with metal-glass assemblies with the photocathodes under study attached to the ends (Fig. 1). The working diameters of the cathode and anode are 18 mm, with a gap between the electrodes of 0.7-1.5 mm.

The heterostructures of the photocathode and the A^3B^5 spin detector were grown on GaAs substrates by molecular beam epitaxy or by metal-organic chemical vapor deposition. An anti-reflective SiO coating was applied over the heterostructures. After growth, the heteroepitaxial structures were cut into discs according to the size of the photocathode assemblies and welded to the glass of the photocathode assembly through the SiO coating using thermal diffusion welding. Then, the GaAs substrate and, in the case of the photocathode, the AlGaAs buffer layer were removed by chemical selective etching. The final stage of the cleaning procedure for both the cathode and anode was carried out in a glove box filled with pure nitrogen, where the cathode and anode were chemically treated in a solution of HCl in isopropyl alcohol [23]. Both cleaned surfaces were activated to a state of effective negative electron affinity by adsorption of cesium and oxygen in an ultra-high vacuum chamber. The photocathode and anode were hermetically fixed on opposite sides of a cylindrical housing made of aluminum oxide ceramic in ultra-high vacuum [24].

When manufacturing photodiodes with multi-alkali photocathodes, the photocathode material was applied to the metal-glass photocathode assembly in a high-vacuum chamber immediately before sealing. In the case of manufacturing photodiodes with a multi-alkali photocathode and A^3B^5-anode, the anode heterostructure was activated by applying cesium and antimony. Photocathodes based on multi-alkali compounds demonstrate the necessary photoemission characteristics for use in the SDPE method: the emission current exceeds 1 μA with an energy spread in the electron beam of 50-100 meV.

To check the polarization properties of Na_2KSb:Cs photocathode, circularly polarized photoluminescence (PL) spectra were measured. Figure 2a shows the circularly polarized PL spectra of the multi-alkali photocathode when illuminated with circularly polarized laser radiation with a photon energy of $h\omega = 1.49$ eV (830 nm), Figure 2b shows the PL polarization degree spectrum. The dependence of the circular polarization degree of PL in Na_2KSb on the incident photon energy is shown in Figure 2c. The degree of PL polarization rapidly decreases with increasing incident radiation energy up to approximately 2.4 eV. However, unlike GaAs, where PL polarization becomes zero [18], in Na_2KSb it remains at a level of about 4% at higher excitation energies. Another important difference from GaAs is that the decline in PL polarization in Na_2KSb occurs at higher excitation energy values, which is related to the difference in the spin-orbit splitting magnitude in Na_2KSb and GaAs (0.55 and 0.34 eV, respectively).

The similarity in the dependence of PL polarization at low excitation energies, as well as the similarity of the band structure of Na_2KSb and GaAs [18] proves that the optical orientation effect is observed in Na_2KSb, this similarity suggests that the selection rules for optical transitions for Na_2KSb and GaAs are the same. The degree of PL polarization in Na_2KSb even at room temperature was found to be 23%, which is close to the theoretical limit of 25%. Assuming the absence of spin scattering during the electron emission process into vacuum, it can be expected that the maximum polarization of photoemitted electrons from Na_2KSb is 45-50%.

3. DETECTOR OF SPIN-POLARIZED ELECTRONS

The idea of a semiconductor spin detector is based on the injection of free electrons into the bottom of the conduction band followed by radiative recombination of an electron with a hole, emitting a quantum of light. The polarization of radiation during the recombination of spin-polarized electrons is also due to the transfer of angular momentum from electrons to light, so the degree of circularly polarized photoluminescence (PL) can indicate the degree of polarization of electrons generated in a photoemitter, and the degree of polarization of cathodoluminescence (CL) can indicate

the degree of polarization of electrons injected from vacuum into the detector anode. In this case, CL refers to radiation generated during the recombination of primary electrons injected into the semiconductor from vacuum, while registration can be performed with spatial resolution.

Semiconductor heterostructures based on the well-known GaAs/Al $_{1-x}$ Ga $_{x}$ As heteropair were studied as a spin detector. Circularly polarized CL spectra, measured during the injection of spin-polarized electrons from a Na $_{2}$ KSb:Cs photocathode with an energy of 1.0 eV, are shown in Fig. 3a.

The maximum CL intensity corresponds to a radiation energy of 1.53 eV (810 nm), which coincides with the bandgap of Al $_{0.11}$ Ga $_{0.89}$ As. The degree of circular polarization of CL radiation was a 4% (Fig. 3b). The dependence of the degree of circular polarization of CL, obtained by injecting spin-polarized electrons from a Na $_{2}$ KSb:Cs photocathode, on the energy of injected electrons in the range of 0.6-4 eV in the spectra and image measurement mode is shown in Fig. 3c. For Na $_{2}$ KSb:Cs, the maximum degree of CL polarization is 9.5% at low kinetic energies (0.6 eV), and it monotonically decreases to approximately 1% as the electron energy increases to 4 eV. When comparing CL polarization for Na $_{2}$ KSb:Cs and GaAs:Cs-O photocathode, the latter was found to be half as much. Assuming that the polarization of photoelectrons from the GaAs cathode is in the range of 20-25% [18], it can be concluded that the polarization of photoelectrons emitted from Na $_{2}$ KSb:Cs lies in the range of 40-50%, which is in good agreement with the polarization degree estimation made from polarized PL measurements.

For practical applications in spin polarimetry, important characteristics of the detector are the Sherman function $S = A / P_0$, where A is the measured asymmetry function with known polarization of the electron beam, P_0 reflects the selectivity of the polarimeter to the electron spin projection, the quality factor (demonstrating the sensitivity of the polarimeter) is determined by the formula $F = S^2 I_{CL} / I_0$, where I_{CL} is the intensity of the registered cathodoluminescence, and I_0 is the current of incident electrons. It is shown that the Sherman function of the detector based on Al $_{0.11}$ Ga $_{0.89}$ As is $S_{eff} \approx 0.3$ [24], and the evaluation of single-channel detection efficiency gives a value of $F \approx 1 \cdot 10^{-3}$. At the same time, the dependence of the degree of circular polarization of CL on the kinetic energy of injected electrons and its maximum value are determined by spin relaxation in the "bulk" of the semiconductor heterostructure, and the external quantum yield of CL is limited by non-radiative recombination. Optimization of the composition and structure, as well as technological parameters of manufacturing spin-detector heterostructures, can significantly increase their efficiency – to parameter values exceeding the level of existing types of detectors in single-channel mode and significantly exceeding them in multi-channel operation mode. Thus, it can be concluded that a spin detector based on semiconductor heterostructures can be successfully used to measure the spin polarization of free

electrons. Unlike a single-channel Mott detector, a semiconductor detector can be used as a multi-channel detector with spatial resolution, which increases efficiency by N_{ch} times, where N_{ch} is the number of channels.

Another type of spin detector, which can also be used in SPES experiments, consists of a ferromagnetic layer/semiconductor heterostructure [25-27]. A spin detector based on the ferromagnet/semiconductor structure is inferior in efficiency to the detector described above; however, it may prove to be more stable under SPES method operating conditions.

4. EXPERIMENTAL SETUP FOR STUDYING SPIN-POLARIZED ELECTRON SCATTERING BY SDSE METHOD

Results on the creation and study of the properties of new spin-polarized sources and free electron spin detectors based on semiconductor heterostructures have allowed us to begin the development and production of a new unique setup for investigating resonant scattering by the SDSE method. A schematic representation of the conceptual multi-chamber ultra-high vacuum setup for studying spin-polarized electron scattering by the SDSE method [28, 29] is shown in Fig. 4. The setup consists of four main chambers: the main chamber (reaction chamber, target chamber); photocathode chamber (source chamber); photocathode growth/preparation chamber (growth & activation chamber); electron spin polarization analysis chamber (spin-detector chamber). A loading (gateway) chamber will be attached to the growth chamber for loading photocathode assemblies. All chambers will have independent pumping means, and the chambers will be separated by gate valves. The base pressure in the main chambers should not exceed 10^{-10} mbar.

The main chamber will house a collision cell for implementing the crossed-beam technique in DEA [30]: a beam of neutral molecules under study, prepared in an effusive source, intersects at right angles with a beam of slow (0-15 eV) longitudinally spin-polarized electrons. In the beam intersection region, negative molecular ions are formed, which decay both through the electron autodetachment channel and through dissociation into neutral and negatively charged fragments. The latter are analyzed using a quadrupole mass spectrometer (mass range 1-300) as a function of electron energy in the probe beam. It should be noted that in the conventional DEA method technique [28, 31], the electron beam characteristics are as follows: beam current of about 1 μA, full width at half maximum (FWHM) of the electron energy distribution 0.4-0.5 eV, accuracy of determining the position of resonances in the electron scattering cross-section ±0.1 eV. The energy scale calibration is mainly performed using the signal of long-lived negative molecular ions SF_6^-, formed by the capture of thermal (zero energy) electrons by sulfur hexafluoride molecules. When using a trochoidal electron

energy monochromator [32, 33], the FWHM value decreases to 30-50 meV; however, the beam current drops to values of the order of nanoamperes, which significantly reduces sensitivity when recording negative ion currents. When studying enantiomers of chiral molecules, the registered value is the signal asymmetry A [11], calculated using the relation $A_{+(-)} = [(I_{\uparrow} - I I_{\downarrow})/(I_{\uparrow} + I_{\downarrow})]_{+(-)}$, where the indices "+" and "-" correspond to two enantiomers (in the simplest case of one chiral center in the molecule), $I = I(\sum)$ - the intensity of the measured negative ion current for a given decay channel as a function of electron energy ($\sum$) in the primary beam when the electron spin direction coincides with its momentum (↑), or is opposite to it (↓).

In the photocathode chamber, a photocathode assembly holder will be installed with the ability to heat up to a temperature of 500 K and cool down to a temperature of 80-90 K. Photocathodes based on both Na_2KSb and GaAs are thin layers on a glass substrate, which allows for photoemission of polarized electrons when the photocathode is illuminated in reflection mode (laser 1) and transmission mode (laser 2), Fig. 4. Lasers 1 and 2 can also be used for optical orientation of molecules in the main chamber. Electrons photoemitted from the cathode are then transferred using electron optics to the high-pressure cell in the main chamber.

The cathode growth/preparation chamber is designed for growing multi-alkali photocathodes by molecular beam or gas-phase epitaxy. For the growth of the multi-alkali compound Na_2KSb/Cs,Sb, sources of Na, K, Sb, as well as Cs for activating the cathode surface are used. Borosilicate glass is used as a substrate, which allows working with the photocathode in both "transmission" and "reflection" modes. The thickness of the active Na_2KSb layer is optimized during the growth process, based on obtaining the maximum photoemission current, which is determined mainly by the depth of light absorption and the diffusion length of minority carriers (photoelectrons). For test measurements, standard GaAs photocathodes (or photocathodes based on A^3B^5 compounds) sealed onto a glass assembly [24] are also planned to be used.

In the chamber for analyzing the spin polarization of electrons scattered from target molecules, semiconductor spin detectors with spatial resolution, previously developed by us [18, 24], will be used. The use of two detectors will allow measuring three components of the spin of scattered electrons.

5. CONCLUSION AND PROSPECTS

The resistance of multi-alkali photocathodes to degradation, as well as their newly discovered property as a source of spin-polarized electrons, make these photocathodes promising for implementing the method of dissociative electron attachment spectroscopy with polarized electrons.

Moreover, preliminary results on the study of strained photocathodes based on Na_2KSb:Cs demonstrate the possibility of obtaining an electron beam with polarization significantly exceeding 50%. Spin-polarized photoemission from Na_2KSb:Cs also opens up the possibility of creating new efficient electron sources for accelerators that simultaneously possess high quantum yield, spin polarization of emitted electrons, longevity, and low emittance.

Spin detectors based on semiconductor structures are optimal for conducting SDEA experiments. Unlike standard Mott detectors, they operate in the low electron energy range (units of eV compared to tens of keV for a Mott detector) – in the electron energy range of the SDEA method, which also prevents discharge ignition. The obtained characteristics of semiconductor spin detectors (Sherman function, efficiency, spatial resolution) turn out to be better than those of a Mott detector, which will allow achieving significantly better statistics in SDEA experiments.

The developed setup will be modular in nature, allowing the experimental scheme to be reconfigured for various tasks. The presented SDEA measurement scheme can be transformed into a method of electron energy loss spectroscopy using a monochromatic beam of spin-polarized electrons to study magnetic and spin-dependent properties of solid surfaces. Based on the Na_2KSb:Cs source, it is possible to manufacture an electron microscope using spin-polarized electrons to study magnetic properties with high spatial resolution, as well as a diffractometer to study the spin-orbit interaction of polarized electrons with surface atoms.

Thus, the method of dissociative electron attachment spectroscopy with spin-polarized electrons being developed should answer the fundamental question about the origin of biological homochirality and the observed chiral asymmetry in the functioning of living matter, in particular, contribute to the understanding of selective action of pharmaceutical drugs at the molecular level, and this method will also allow the development of surface-sensitive spin-dependent electron-spectroscopic research methods, including for application of expected results in relevant areas of spintronics.

FUNDING

This work was supported by the Russian Science Foundation (project 22-12-20024 (r-9)).

CONFLICT OF INTERESTS

The authors declare that they have no conflict of interest.

REFERENCES

1. *Blum K., Kleinpoppe H.* // Adv. At. Mot. Phys. 1983. V. 19. P. 187.
https://doi.org/10.1016/S0065-2199(08)60254-7

2. *Dellen A*. // J. Phys. B: At. Mol. Opt. Phys. 1995. V. 28. P. 4867.
https://doi.org/10.1088/0953-4075/28/22/017

3. *Blum K., Thompson D.* // J. Phys. B. 1989. V. 22. P. 1823.
https://doi.org/10.1088/0953-4075/22/11/016

4. *Mason N.J.* Spin Dependent Electron Scattering from Oriented Molecules: An Experimental Appraisal // Polarized Electron/Polarized Photon Physics. Boston, MA: Springer US, 1995. P. 209.

5. *Farago P.S.* // J. Phys. B: At. Mol. Phys. 1980. V. 13. P. L567.
https://doi.org/10.1088/0022-3700/13/18/004

6. *Blum K.* Electron Scattering from Chiral Molecules // Coherence in Atomic Collision Physics / Ed. By H. J. Beyer et al. New York: Springer Science+Business Media, 1988. P. 89.
https://doi.org/10.1007/978-1-4757-9745-9_3

7. *Veste F., Ulbrich T.L.V., Krauch H.* // Naturwissenschaften. 1959. V. 46. P. 68.
https://doi.org/10.1007/BF00599091

8. *Beerlage M.J.M., Farago P.S., Van der Wiel M.J.* // J. Phys. B: At. Mol. Phys. 1981. V. 14. P. 3245. https://doi.org/10.1088/0022-3700/14/17/027

9. *Trantham K. W., Johnston M. E., Gay T. J.* // J. Phys. B: At. Mol. Opt. Phys. 1995. V. 28. L543.
https://doi.org/10.1088/0953-4075/28/17/004

10. *Mayer S., Nolting C., Kessler J.* // J. Phys. B: At. Mol. Opt. Phys. 1996. V. 29. P. 3497.
https://doi.org /10.1088/0953-4075/29/15/021

11. *Dreiling J.M., Lewis F.W., Gay T.J.* // J. Phys. B: At. Mol. Opt. Phys. 2018. V. 51. 21LT01.
https://doi.org /10.1088/1361-6455/aae1bd

12. *Sanche L., Schulz G.J.* // Phys. Rev. A. 1972. V. 5. P. 1672.
https://doi.org/10.1103/PhysRevA.5.1672

13. *Dreiling J.M., Gay T.J.* // Phys. Rev. Lett. 2014. V. 113. P. 118103.
https://doi.org/10.1103/PhysRevLett.113.118103

14. *Dreiling J.M., Lewis F.W., Mills J.D., Gay T.J.* // Phys. Rev. Lett. 2016. V. 116. P. 093201.
https://doi.org/10.1103/PhysRevLett.116.093201

15. *Bakin V.V., Pakhnevich A.A., Zhuravlev A.G., Shornikov A.N., Akhundov I.O., Tereshechenko O.E., Alperovich V.L., Scheibler H.E., Terekhov A.S.* // e-J. Surf. Sci. Nanotech. 2007. V. 5. P. 80.

https://doi.org/10.1380/ejssnt.2007.80
16. *Meier F., Zakharchenya B.P.* Optical Orientation. Amsterdam, Oxford, New York, Tokyo: North-Holland, 1984.
17. *Michizono S.* // Nat. Rev. Phys. 2019. V. 1. P. 244. https://doi.org/10.1038/s42254-019-0044-4
18. *Rusetsky V.S., Golyashov V.A., Eremeev S. V., Kustov D.A., Rusinov I.P., Shamirzaev T.S., Mironov A.V., Demin A.Yu., Tereshchenko O.E.* // Phys. Rev. Lett. 2022. V. 129. P. 166802. https://doi.org/10.1103/PhysRevLett.129.166802
19. *Tereshchenko O.E., Golyashov V.A., Rusetsky V.S., Mironov A.V., Demin A.Y., Aksenov V.V.* // J. Synchrotron Radiat. 2021 V. 28. P. 864. https://doi.org/10.1107/S1600577521002307
20. *Golyashov V.A., Rusetsky V.S., Shamirzaev T.S., Dmitriev D.V., Kislykh N.V., Mironov A.V., Aksenov V.V., Tereshchenko O.E.* // Ultramicroscopy. 2020. V. 218. P. 113076. https://doi.org/10.1016/j.ultramic.2020.113076
21. *Rodionov A.A., Golyashov V.A., Chistokhin I.B., Jaroshevich A.S., Derebezov I.A., Haisler V.A., Shamirzaev T.S., Marakhovka I.I., Kopotilov A.V., Kislykh N.V., Mironov A.V., Aksenov V.V., Tereshchenko O.E.* // Phys. Rev. Appl. 2017. V. 8. P. 034026. https://doi.org/10.1103/PhysRevApplied.8.034026
22. *Tereshchenko O.E., Golyashov V.A., Rodionov A.A., Chistokhin I.B., Kislykh N.V., Mironov A.V., Aksenov V.V.* // Sci. Rep. 2017. V. 7. P. 16154. https://doi.org/10.1038/s41598-017-16455-6
23. *Tereshchenko O.E., Chikichev S.I., Terekhov A.S.* // J. Vacuum Sci. Technol. A. 1999. V. 17. P. 2655. https://doi.org/10.1116/1.581926
24. *Tereshchenko O.E., Golyashov V.A., Rusetsky V.S., Kustov D.A., Mironov A.V., Demin A.Yu.* // Nanomaterials. 2023. V. 13. P. 422. https://doi.org/10.3390/nano13030422
25. *Li X., Tereshchenko O.E, Majee S., Lampel G., Lassailly Y., Paget D., Peretti J.* // Appl. Phys. Lett. 2014. V. 105. P. 052402. https://doi.org/10.1063/1.4892073
26. *Tereshchenko O.E., Lamine D., Lampel G., Lassailly Y., Li X., Paget D., Peretti J.* // J. Appl. Phys. 2011. V. 109. P. 113708. https://doi.org/10.1063/1.3592976.
27. *Tereshchenko O.E., Golyashov V.A., Eremeev S.V., Maurin I., Bakulin A. V., Kulkova S.E., Aksenov M.S., Preobrazhenskii V.V., Putyato M.A., Semyagin B.R., Dmitriev D.V., Toropov A.I., Gutakovskii A.K., Khandarkhaeva S.E., Prosvirin I.P., Kalinkin A.V., Bukhtiyarov V.I., Latyshev A.V.* // Appl. Phys. Lett. 2015. V. 107. P. 123506. https://doi.org/10.1063/1.4931944
28. *Khvostenko V.I.* Mass spectrometry of negative ions in organic chemistry. Moscow: Nauka, 1981.

29. *Christophorou L.G.* Electron-molecule interactions and their applications. Orlando: Academic Press, 1984.
30. *Illenberger E., Momigny J.* Gaseous molecular ions. An introduction to elementary processes induced by ionization. Steinkopff Verlag Darmstadt: Springer-Verlag, 1992.
31. *Pshenichnyuk S.A., Asfandiarov N.L., Vorobyev A.S., Matejcik S.* // UFN. 2022. V. 192. P. 177. https://doi.org/10.3367/UFNr.2021.09.039054
32. *Stamatovic A., Schulz G.J.* // Rev. Sci. Instrum. 1968. V. 39. P. 1752. https://doi.org/10.1063/1.1683220
33. *Asfandiarov N.L., Pshenichnyuk S.A., Falko V.S., Lomakin G.S.* // PTE. 2013. V. 56. P. 86. https://doi.org/10.7868/S0032816213010035

FIGURE CAPTIONS

Fig. 1. **a –** Photograph of the photodiode from the photocathode side; **b** – schematic representation of the photodiode in cross-section and the principle of spin-polarized electron generation and detection; **c –** photograph of the anode.

Fig. 2. **a** – Circularly polarized (σ+, σ-) components of the photoluminescence spectra of the Na_2KSb:Cs photocathode when illuminated with circularly polarized light with energy 1.49 eV (830 nm); the peak at photon energy 1.42 eV corresponds to the band gap of Na_2KSb; **b** – corresponding spectrum of the degree of circular polarization of PL, defined as $P_{PL} = (I\sigma^+ - I\sigma-)/(I\sigma^+ + I\sigma^-)$; **c** – dependence of the degree of circular polarization of PL emission for Na_2KSb on the incident photon energy.

Fig. 3. a – Circularly polarized (σ^+, σ^-) components of the cathodoluminescence spectra, measured during injection of spin-polarized electrons emitted from the Na_2KSb:Cs photocathode at an accelerating voltage of 1.0 V, into the anode heterostructure $Al_{0.11}Ga_{0.89}As$; **b** – degree of circular polarization of CL, defined as $P_{CL} = (I\sigma^+ - I\sigma^-)/(I\sigma^+ + I\sigma^-)$; **c** – comparative dependences of the degree of circular polarization of CL on the energy of injected spin-polarized electrons from the Na_2KSb:Cs photocathode in the mode of measuring spectra and images.

Fig. 4. Schematic representation of a multi-chamber ultra-high vacuum installation for studying the scattering of spin-polarized electrons by dissociative electron attachment spectroscopy.

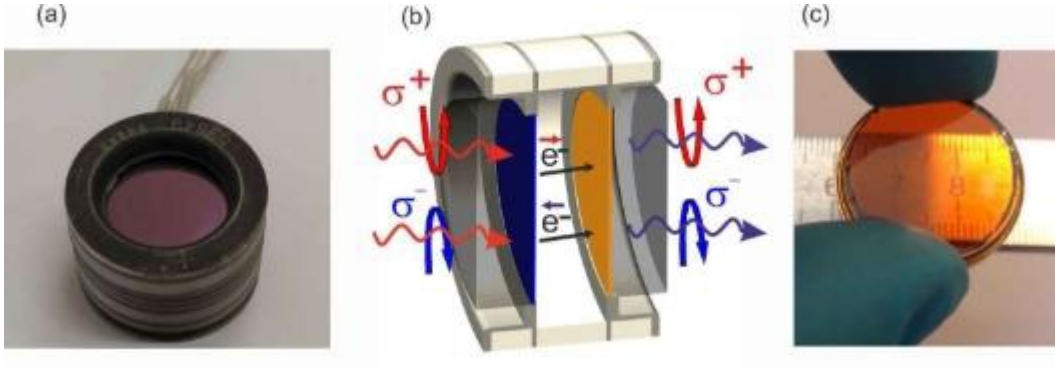

Fig. 1.

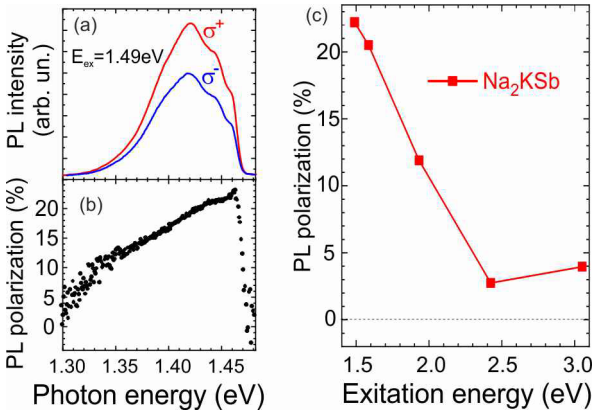

Fig. 2.

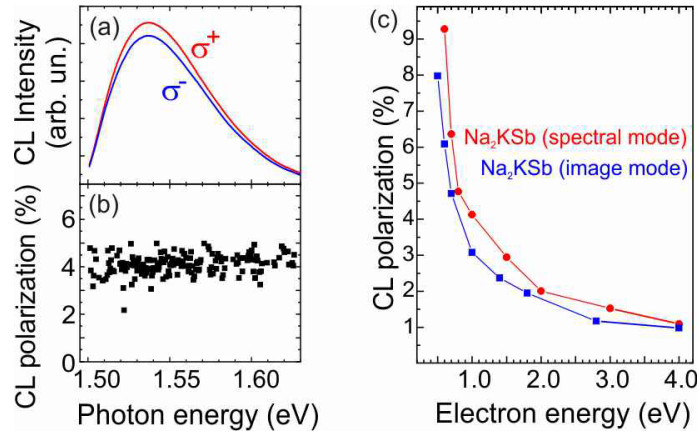

Fig. 3.

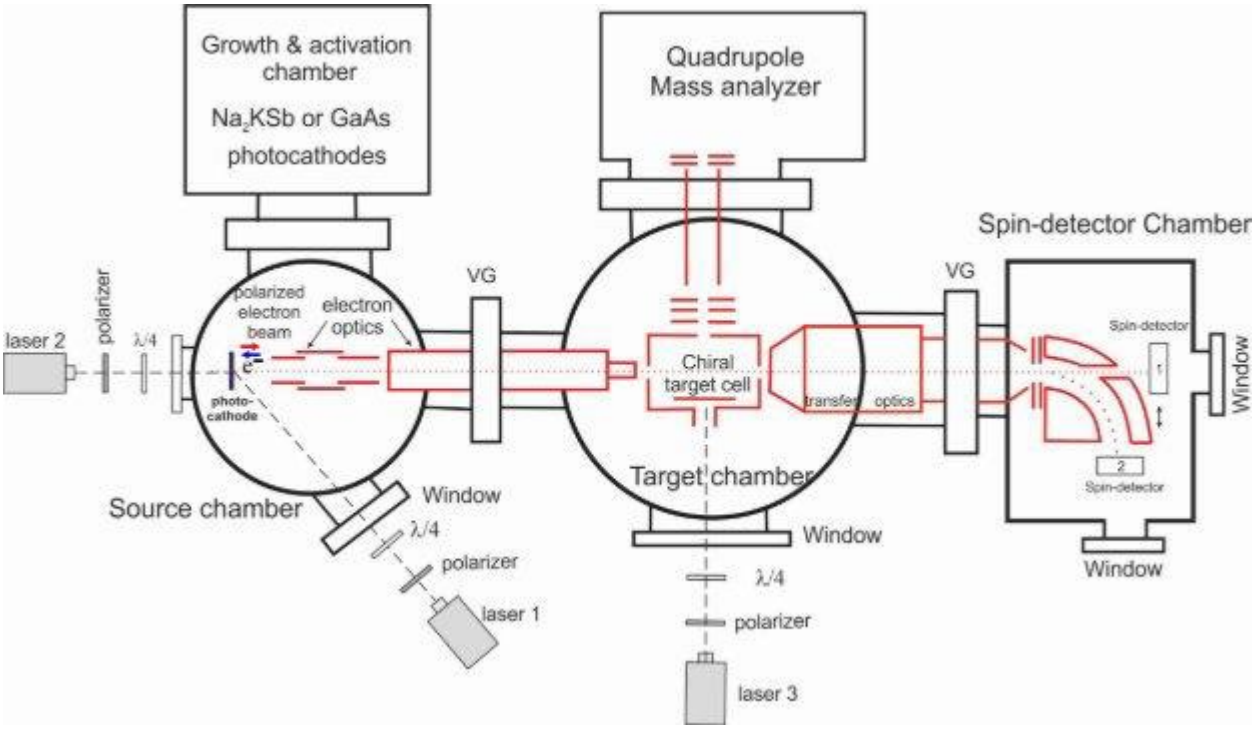
Growth & activation chamber
Na2KSb or GaAs photocathodes
Quadrupole Mass analyzer
Spin-detector Chamber
laser 2
polarizer
λ/4
polarized electron beam
electron optics
photo-cathode
VG
Chiral target cell
transfer optics
VG
Spin-detector
Window
Source chamber
Window
λ/4
polarizer
laser 1
Target chamber
Window
λ/4
polarizer
laser 3
Window

Fig. 4.